

## Temperature dependence of Raman spectra in single-walled carbon nanotube rings

Li Song,<sup>1,a),b)</sup> Wenjun Ma,<sup>1</sup> Yan Ren,<sup>1</sup> Weiya Zhou,<sup>1</sup> Sishen Xie,<sup>1,a),c)</sup> Pingheng Tan,<sup>2</sup> and Lianfeng Sun<sup>3</sup>

<sup>1</sup>Beijing National Laboratory for Condensed Matter Physics, Institute of Physics, Chinese Academy of Sciences, Beijing 100080, People's Republic of China

<sup>2</sup>National Laboratory for Superlattices and Microstructures, Beijing 100083, People's Republic of China

<sup>3</sup>National Center for Nanoscience and Nanotechnology, Beijing 100080, People's Republic of China

(Received 3 December 2007; accepted 14 February 2008; published online 25 March 2008)

The temperature-dependent Raman frequency shift in single-walled carbon nanotube (SWCNT) rings in the range of 80–550 K is investigated. We observe that the frequency decreases with increasing temperature for all Raman peaks of the nanotube rings. Furthermore, compared to the nanotubes with linear structure, the temperature coefficients of the radial breathing mode and G-mode frequencies of the nanotube rings are much smaller, which means the nanotube rings have more stable thermal ability. We attribute the better thermal stability to the high bending strain energy along the nanotube rings induced by the sidewall curvature. © 2008 American Institute of Physics. [DOI: 10.1063/1.2891870]

Since their discovery, carbon nanotubes (CNTs) have been predicted to be the most reliable components of the next generation electronics due to their extraordinary electrical properties.<sup>1</sup> Moreover, thermal stability and temperature-dependence behaviors are very important for such CNT-based devices.<sup>2,3</sup> In this case, resonance Raman scattering should be a very effective and nondestructive tool for detecting nanotube's properties. Specially, the temperature-dependent Raman spectra in CNTs can allow us to understand their fine structure information and properties, such as atomic bond structure, thermal expansion, specific heat, and thermal conductivity.<sup>4–9</sup> A temperature variations of the Raman spectra in multi-walled CNTs (MWCNTs) was investigated by Huang *et al.*<sup>4</sup> It was found that the frequency decreases with increasing temperature for the tangential stretching G-mode (GM), D-band, and D\*-mode peaks. Compared to MWCNTs, the temperature coefficient of the GM in single-walled carbon nanotubes (SWCNTs) was much larger.<sup>5</sup> Ravivkar *et al.* reported that the temperature induced softening of the intra- and intertubular bonds contributed significantly to the temperature shift of frequency in the radial breathing mode (RBM).<sup>6</sup> On the other hand, as one surprising superstructure, many theoretical reports have predicted that nanotubes with an annular geometry should become a promising material for realization of nanoelectronics.<sup>10–12</sup> However, until now, due to the challenge in their preparation, few works have been reported concerning the thermal properties in such nanotube rings.

Recently, we have selectively synthesized SWCNT rings with high yield.<sup>13,14</sup> In this letter, we further report a study of the temperature-dependent Raman spectra of these SWCNT rings. It is found that the frequency decreases with increasing temperature for all peaks of the nanotube ring's Raman-active modes. Meanwhile, the variable temperature

Raman spectra of linear SWCNTs is also comparatively investigated. Note that compared to the linear nanotubes the temperature coefficient of the RBM and GM frequencies in the nanotube rings are much smaller, which means the nanotube rings have better thermal stability. We suggest that the high bending strain energy along the ring curvature releases the temperature induced softening behavior of the CNT rings.

The detail measurements are described in our supporting information.<sup>15</sup> Figure 1 shows the variations of the Raman spectra of the SWCNT rings at different temperatures. At low frequency region, the Raman shifts of four RBM peaks with temperature were shown in Fig. 1(a), as well as the peak came from the silicon substrate (marked by asterisks in

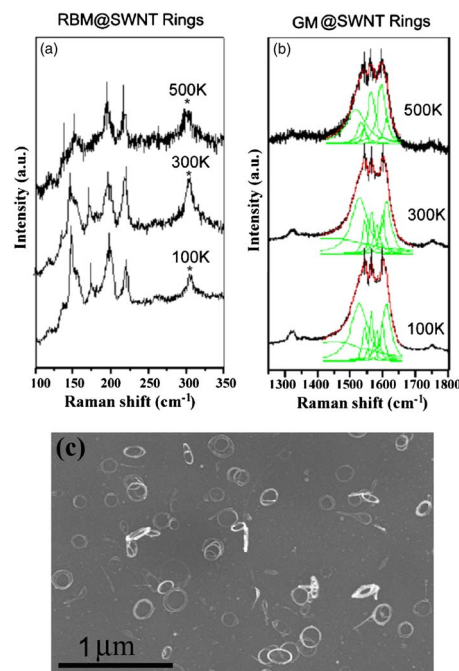


FIG. 1. (Color online) Raman spectra of RBM (a) and GM (b) of the SWCNT rings at temperature of 100, 300, and 500 K, respectively. (c) A typical SEM image of the SWCNT rings samples.

<sup>a)</sup> Authors to whom correspondence should be addressed.

<sup>b)</sup> Present address: Center for NanoScience and Department of Physics, LMU, Munich 80539, Germany. Electronic mail: li.song@physik.uni-muenchen.de

<sup>c)</sup> Electronic mail: sxxie@aphy.iphy.ac.cn.

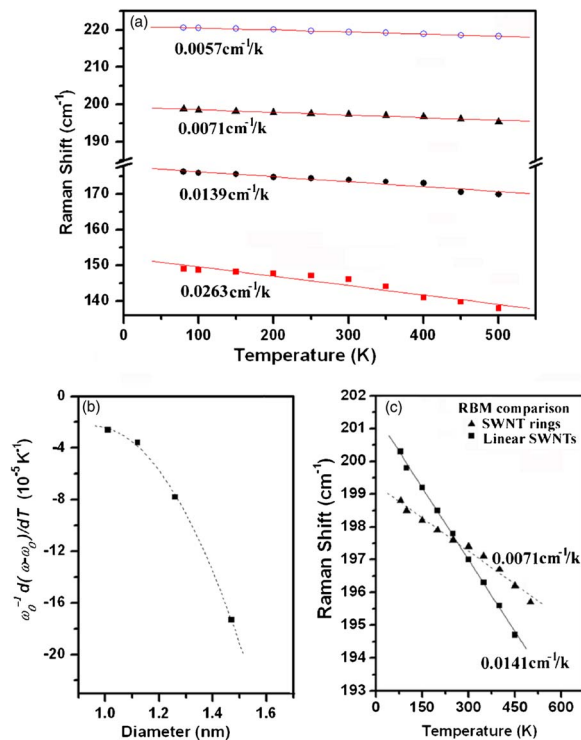


FIG. 2. (Color online) (a) RBM frequencies shift as a function of temperature for the SWCNT rings. The lines are linear fitting results for obtaining the temperature dependence of the frequency. (b) The relation between the normalized temperature coefficient of RBM frequencies and the diameter of SWCNTs inside the rings. The dash lines are the fits with quadratic curve. (c) The comparison of the temperature-induced RBM frequency variations between the SWCNT rings and the linear SWCNTs, which have the similar diameter at room temperature.

spectrum, the detail is shown in the supporting information). At high frequency region, three GM peaks were considered for the next analysis (the peak separations using multi-Lorentzian lines), as shown in Fig. 1(b). It is easy to find that the frequencies of all the Raman peaks of the nanotube rings, including RBM and GM, downshift simultaneously with increasing temperature, which is consistent with the previous reports about SWCNTs.<sup>6,7</sup> The intensity of the Raman peaks decline a little with the temperature increasing. Figure 1(c) shows the typical morphology of the used specimens in our experiments. The SWCNT rings show the diameter of about 100–200 nm. Some of the rings fell to the substrate (gray), while some adhered at the edge (bright). Moreover, as the compared case, the variable temperature Raman spectra of the linear-structure SWCNTs were investigated under same experimental conditions, as shown in the supporting information.

Furthermore, the temperature-dependent frequencies of four RBM peaks of the nanotube rings are displayed in Fig. 2(a). Obviously, the temperature variations of each RBM frequency can be fitted well by a straight line. The inserted slope values clear show that the temperature coefficients of RBM Raman frequency shift (i.e.,  $d\omega/dT$ ) are quite different. The RBM peak relative to CNT with the larger diameter has the larger frequency downshift. In order to further analyze the relation between the temperature coefficient of each RBM frequency and nanotube diameter, we normalized the temperature coefficients by  $\omega_0^{-1}d(\omega-\omega_0)/dT$ , where the diameter ( $d$ , nm) were determined by the relation of  $d=224/\omega_{\text{RBM}}$ ,  $\omega_{\text{RBM}}$  is each RBM frequency at 300 K. The

normalized temperature coefficient as a function of diameter was plotted in Fig. 2(b) and it could be well fit by a quadratic curve. Figure 2(c) shows the comparison of the temperature-induced RBM frequency shift between the SWCNT rings and the linear-structure SWCNTs, which show the similar diameter at room temperature. It is noting that the temperature coefficient of RBM frequency shift for the SWCNT rings is much smaller than the linear SWCNTs, which indicates more stable thermal ability in the nanotube rings.

Several theories have been reported for explaining the reason of the temperature-induced RBM frequency shift in carbon nanotubes. According to the force constant model,<sup>16</sup> the RBM frequency of SWCNTs can be expressed as

$$\omega_{\text{RBM}} = \frac{2a_{\text{C-C}}\sqrt{\Phi}}{\sqrt{md}}, \quad (1)$$

where  $a_{\text{C-C}}$  is the carbon-carbon bond length,  $m$  is the mass of carbon atom, and  $d$  is the diameter of nanotube.  $\Phi$  denotes the C–C bond-stretching force constant, and can be expressed as

$$\Phi = \frac{9}{16}\phi_r^{(1)} + \frac{27}{8}\phi_r^{(2)} + \frac{9}{4}\phi_r^{(3)} + \frac{63}{8}\phi_r^{(4)}, \quad (2)$$

where  $\phi_r^{(i)}$  is the C–C bond-stretching force constant between carbon atom and the its nearest neighbor. In this model, it is easy to know that RBM frequency has a close relation with the C–C bond length, nanotube diameter and the force constant. Furthermore, our experimental temperatures (up to 550 K) are sufficiently below the Debye temperature of the graphite layer (2500 K), the thermal expansion coefficient of  $a_{\text{C-C}}$  is extremely small and has very small contribution to the RBM frequency.<sup>17</sup> The change in the diameter of the nanotube  $d$  also can be neglected in our temperature range.<sup>18</sup> Therefore, the temperature-dependent force constant should play the main role for the RBM frequency shift of the SWCNT rings. It is easy to expect that the C–C bond-stretching force constant should decrease with the temperature increasing, due to the softened C–C bond at the higher temperature. In our above observation, the smaller RBM Raman frequencies downshift for the small diameter nanotubes means the smaller temperature dependence of the force constants for the smaller nanotubes inside the SWCNT rings. Moreover, nanotube ring can be considered as bending a straight nanotube bundles elastically and closing upon itself by van der Waals interaction. Therefore, the annular geometry of nanotube ring induces the change of C–C bond conformation along the ring circumference, including the C–C bond-uniaxial elongation and compression. Furthermore, the high bending strain energy should make the softening of the C–C bond more difficult, which means the C–C bond stretching force constant for the nanotube rings has less dependence on temperature compared to the straight nanotubes. Therefore, the temperature coefficient of RBM frequency shift for the SWCNT rings is much smaller than the linear-structure nanotubes in our investigations.

We also carried similar analyses on the three GM peaks of the SWCNT rings, as shown in Fig. 3(a)–3(c). It is found that these GM frequencies exhibit nonlinear decrease with increasing temperature, which can be fitted well by three second-order curves. The temperature coefficients of the three GM frequencies shift are shown as the insert data, and there no remarkable different between these values. In terms

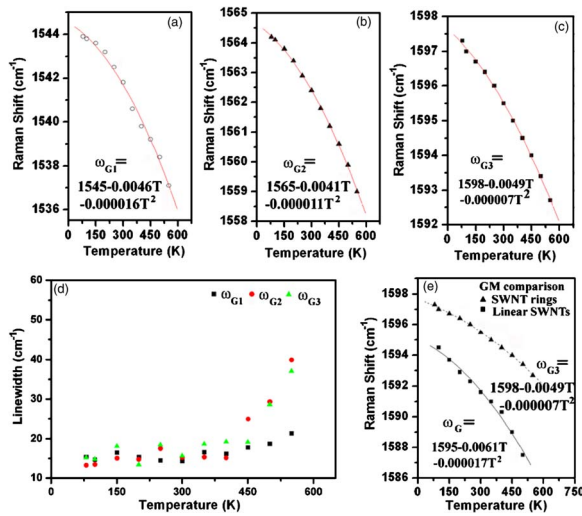


FIG. 3. (Color online) (a)–(c)  $G$  modes frequencies shift as a function of temperature for the SWCNT rings. The solid lines are the fits with second-order formula. (d) Linewidth dependence of the  $G$  peaks on the temperature for the SWCNT rings. (e) The comparison of the temperature-induced  $GM$  frequency variations between the SWCNT rings and the linear SWCNTs.

of the theoretic studies,<sup>19,20</sup> the anharmonic term in Lagrangian for the lattice vibrating of carbon nanotube could make its Raman shift have a linear ( $T$ ) and second-order ( $T^2$ ) relation with temperature, and the temperature dependence of Raman frequency shift could be well represented by the following relation:

$$\omega = \omega_0 - \alpha_1 T - \alpha_2 T^2, \quad (3)$$

where  $\omega_0$  is the frequency when temperature is extrapolated to 0 K, and  $\alpha_1$  and  $\alpha_2$  are the first- and second-order  $T$  coefficients, respectively. However, in our obtained results, we found that the RBM frequencies of SWCNT rings show the linear relation with temperature, while the  $GM$  frequencies have better fitted the temperature dependence with the second-order rather than linear formula. This suggests that third- and fourth-order anharmonic terms in the lattice potential energy of the nanotube rings, which determine the second-order coefficient  $\omega_2$  in Eq. (3), have play a role in the temperature-dependent  $GM$  peaks shift, even though this anharmonic contribution is quite small due to the sample temperature far below the Debye temperature of the graphite.<sup>21,22</sup>

Further confirmation could be expected in the full width at half maximum (FWHM) of  $GM$  peaks, because the FWHM sensitively changes with temperature due to the contribution of anharmonic terms. Figure 3(d) shows the FWHM dependence of the  $G$  peaks on the temperature for the SWCNT rings. It is observed that there have no remarkable changes in the FWHM when temperature below 400 K while the FWHM increase quickly with temperature increasing from 400 to 500 K, which indicates the third- and fourth-order anharmonic terms play an obvious effect for the nanotube ring's  $GM$  Raman frequency only when the specimens temperature is above 400 K. Figure 3(e) shows the comparison of the temperature-induced  $GM$  frequency shift between the SWCNT rings and the linear-structure SWCNTs. It indicates that the temperature coefficient of  $GM$  Raman frequency shift for the SWCNT rings is smaller than the linear SWCNTs. This further confirms the SWCNT rings have more stable thermal properties due to the bending strain along the ring curvature.

In conclusion, we have presented experimental results describing the temperature variation in the Raman spectra of SWCNT rings, as well as compared with those of linear-structure nanotubes. We found that the frequency decreases with increasing temperature for RBM and  $GM$  peaks of the nanotube rings. Furthermore, the observed spectra indicated that the temperature coefficients of the RBM and  $GM$  frequencies in the nanotube rings are much smaller than those of the linear nanotubes, which are ascribe to the high bending strain along the nanotube rings induced by the ring curvature. The good thermal stability of SWCNT rings should give advantage for building up the next generation nanometer-scale electric circuits.

Financial support came from National Natural Science Foundation of China (Grant Nos. 10334060 and 50572119) and “973” National Key Basic Research Program of China (Grant No. 2005CB623602). L. Song acknowledges support of the Alexander Von Humboldt Foundation. We thank Professor Kotthaus (LMU), Professor Holleitner (WSI, TUM), and Professor Hartschuh (LMU) for their useful discussions.

- <sup>1</sup>S. J. Tans, R. M. Verschueren, and C. Dekker, *Nature (London)* **393**, 49 (1998).
- <sup>2</sup>Y. K. Kwon, D. Tománek, and S. Iijima, *Phys. Rev. Lett.* **82**, 1470 (1998).
- <sup>3</sup>J. Kong, N. R. Franklin, C. W. Zhou, M. G. Chapline, S. Peng, K. Cho, and H. J. Dai, *Science* **287**, 622 (2000).
- <sup>4</sup>F. Huang, K. Yue, P. Tan, S. Zhang, Z. Shi, X. Zhao, and Z. Gu, *J. Appl. Phys.* **84**, 4022 (1998).
- <sup>5</sup>H. D. Li, K. T. Yue, Z. L. Lian, L. X. Zhou, S. L. Zhang, Z. J. Shi, Z. N. Gu, B. B. Liu, R. S. Yang, G. T. Zou, and S. Iijima, *Appl. Phys. Lett.* **76**, 2053 (2000).
- <sup>6</sup>N. R. Naravikar, P. keblinski, A. M. Rao, M. S. Dresselhaus, L. S. Schadler, and P. M. Ajayan, *Phys. Rev. B* **66**, 235424 (2002).
- <sup>7</sup>L. J. Ci, Z. P. Zhou, L. Song, X. Q. Yan, D. F. Liu, H. J. Yuan, Y. Gao, J. X. Wang, L. F. Liu, W. Y. Zhou, G. Wang, and S. S. Xie, *Appl. Phys. Lett.* **82**, 3098 (2003).
- <sup>8</sup>Z. P. Zhou, X. Y. Dou, L. J. Ci, L. Song, D. F. Liu, Y. Gao, J. X. Wang, L. F. Liu, W. Y. Zhou, and S. S. Xie, *J. Phys. Chem. B* **110**, 1206 (2006).
- <sup>9</sup>Y. Y. Zhang, L. M. Xie, J. Zhang, Z. Y. Wu, and Z. F. Liu, *J. Phys. Chem. C* **111**, 14031 (2007).
- <sup>10</sup>R. C. Haddon, *Nature (London)* **388**, 31 (1997).
- <sup>11</sup>R. Martel, H. R. Shea, and Ph. Avouris, *Nature (London)* **398**, 299 (1999).
- <sup>12</sup>S. Latil, S. Roche, and A. Rubio, *Phys. Rev. B* **67**, 165420 (2003).
- <sup>13</sup>L. Song, L. J. Ci, L. Lv, Z. P. Zhou, X. Q. Yan, D. F. Liu, H. J. Yuan, Y. Gao, J. X. Wang, L. F. Liu, X. W. Zhao, Z. X. Zhang, X. Y. Dou, W. Y. Zhou, G. Wang, C. Y. Wang, and S. S. Xie, *Adv. Mater. (Weinheim, Ger.)* **16**, 1529 (2004).
- <sup>14</sup>L. Song, L. J. Ci, L. F. Sun, C. H. Jin, L. F. Liu, W. J. Ma, D. F. Liu, X. W. Zhao, S. D. Luo, Z. X. Zhang, Y. J. Xiang, J. J. Zhou, W. Y. Zhou, Y. Ding, Z. L. Wang, and S. S. Xie, *Adv. Mater. (Weinheim, Ger.)* **18**, 1817 (2006).
- <sup>15</sup>See EPAPS Document No. E-APPLAB-92-039810 for experimental procedures, SEM, and Raman spectra of line-structure SWNTs, and Raman spectra recorded from the silicon substrate. For more information on EPAPS, see <http://www.aip.org/pubservs/epaps.html>.
- <sup>16</sup>R. A. Jishi, L. Venkataraman, M. S. Dresselhaus, and G. Dresselhaus, *Chem. Phys. Lett.* **209**, 77 (1993).
- <sup>17</sup>Y. Maniwa, R. Fujiwara, H. Kira, H. Tou, H. Kataura, Sh. Suzuki, Y. Achiba, E. Nishibori, M. Takata, M. Sakata, A. Fujiwara, and H. Suetsumu, *Phys. Rev. B* **64**, 241402 (2001).
- <sup>18</sup>Y. Maniwa, R. Fujiwara, H. Kira, H. Tou, E. Nishibori, M. Takata, M. Sakata, A. Fujiwara, X. Zhao, S. Iijima, and Y. Ando, *Phys. Rev. B* **64**, 073105 (2001).
- <sup>19</sup>M. Balkanski, R. F. Wallis, and E. Haro, *Phys. Rev. B* **28**, 1928 (1983).
- <sup>20</sup>H. Herchen and M. A. Cappelli, *Phys. Rev. B* **43**, 11740 (1991).
- <sup>21</sup>W. J. Borer, S. S. Mitra, and K. V. Namjoshi, *Solid State Commun.* **9**, 1377 (1971).
- <sup>22</sup>P. Tan, Y. Deng, Q. Zhao, and W. Heng, *Appl. Phys. Lett.* **74**, 1818 (1999).